Clinical & Experimental Immunology
The Journal of Translational Immunology

Clinical and Experimental Immunology ORIGINAL ARTICLE doi:10.1111/j.1365-2249.2008.03841.x

Giant cell formation in sarcoidosis: cell fusion or proliferation with non-division?

T. C. M. Th. van Maarsseveen, W. Vos and P. J. van Diest
Department of Pathology, VU University Medical Center, Amsterdam, the Netherlands

Accepted for publication 29 October 2008
Correspondence: T. C. M. Th. van Maarsseveen, Department of Pathology, VU University Medical Center, De Boelelaan 1117, 1081 HV Amsterdam, the Netherlands.
E-mail: ac.vanmaarsseveen@vumc.nl

Summary

Granulomas are inflammatory reactions featuring macrophages, epithelioid, T and multi-nucleated giant cells (MGC). Giant cells are present in a number of granulomatous reactions, but little is known about their formation and function, especially in man. We studied MGC in the granulomatous disorder sarcoidosis. *In situ* labelling of lymph nodes by means of [^{3}H]-thymidine showed that proliferation and non-division of epithelioid cells leading towards giant cells was not observed in these granulomas. However, [^{3}H]-uridine incorporation showed MGC with labelled as well as unlabelled nuclei in the same cell, pointing to a process of fusion of epithelioid cells to form giant cells. Apoptotic bodies were incidentally found in granulomas. A novel finding was that such bodies were statistically more often found in the close vicinity of MGC, but not within these cells. These apoptotic cells appeared to be CD4$^+$ lymphocytes or histiocytes. CD44 and CCR-5 involved in the process of fusion were expressed in MGC. In conclusion, MGC in sarcoidosis derive by cell fusion rather than by proliferation and non-division, and seem to play an active role in the induction of apoptosis in granulomas.

Keywords: apoptosis, multi-nucleated giant cell, radio nucleotide incorporation, sarcoidosis

Introduction

Multi-nucleated giant cells (MGC) are regular features of granulomatous inflammation. Evidence has accumulated that MGC arise mainly by fusion of monocytes, macrophages or epithelioid histiocytes [1–3], but some rate of DNA synthesis, resulting in nuclear division without cytoplasmic separation, could not be excluded in these cells [4–8]. Giant cells have been divided into the so-called Langhans type (LH-MGC) or the foreign body type (FB-MGC). Although these cells possess some different morphological features, there is no fundamental difference in function, as has been suggested [9], but different functions of these cells have also been reported [5,10–13]. In addition, human macrophages can be transformed into FB-MGC from a LH-MGC in tissue culture by means of different cytokines [14]. Therefore, controversy still exists in reports concerning the evolution from monocytes/macrophages to giant cells. The significance of MGC in granulomas has been determined from experimental studies on tissues from rats or mice, but such investigations cannot be carried out in humans. Therefore, peripheral leucocytes recovered from patients were used for such investigations [10,15,16]. However, in MGC-related diseases such as tuberculosis, lepra or foreign body granulomas, mediastinal biopsies are not routine, so for practical reasons these diseases did not qualify for the present study. Reports of giant cell formation in human tissue are scarce [10,17]; however, for diagnostic reasons mediastinal lymph node biopsies could be retrieved from patients suspected for sarcoidosis. Hence, we focused on this inflammatory process, in which both types of giant cells can be seen [18]. From earlier experiments [19,20], radio-labelling revealed DNA and RNA synthesis in epithelioid cells from fresh lymph node slices from sarcoidosis patients. For the present study, the same sections were re-evaluated for radio-labelled MGC to answer the 'proliferation or fusion' question, expanded with immunohistochemistry for cell fusion factors CD44 and CCR-5. Because the life cycle of mononuclear cells within the granulomatous tissue includes death [18], apoptosis as a morphologically distinct form of programmed cell death [21–23] was also studied quantitatively and topographically.

Material and methods

Patients, tissue samples and differentiation of MGC

Pathological specimens of subclavicular or mediastinal lymph nodes obtained from 71 patients with proven sarcoidosis were retrieved from the archives of the Department of Pathology, VU University Medical Center. Diagnosis was based on radiological, clinical and histopathological criteria. The nodes were fixed in 4% formaldehyde and embedded in paraffin wax. In one 5-μm-thick haematoxylin and eosin (H&E)-stained section of these lymph nodes, at least 30 granulomas were screened for both types of MGC. A cell with at least four nuclei was considered to be MGC in accordance with previously established criteria [6,9,10,24]. The average number of LH-MGC (in which the nuclei are distributed around the periphery of the cell) and/or FB-MGC (with nuclei haphazardly throughout the cytoplasm) was expressed as number of LH- or FB-/total number of observed granulomas (LH/gr or FB/gr) [18].

Radio-labelling studies

From earlier experiments, in which [^{3}H] nucleotides were applied on fresh lymph node slices from sarcoidosis patients, the radio-labelled granuloma sections were re-evaluated [19,20]. In brief, fresh lymph nodes from sarcoidosis patients were obtained by mediastinoscopy, performed as part of the routine clinical investigation. Immediately after operation, 500 μm-thick slices from the lymph nodes were pulse-labelled for 3 h with tritiated thymidine ([^{3}H] thymidine) at 4 μCi/ml in RPMI-1640 medium supplemented with 20% inactivated pooled human serum (under 95% O_2 and 5% CO_2). As a control of DNA synthesizing properties, tritiated uridine ([^{3}H]-uridine) radio-labelling was applied on consecutive slices to demonstrate RNA synthesis, which excludes negative tissue culture influence. Next, serial 5 μm paraffin sections were made perpendicularly to the cut surface of the sliced lymphoid tissue and overlaid with Ilford G-5 photographic emulsion for 2 weeks. After development and fixation of the emulsion, H&E staining was performed. Cell nuclei were screened for grains, regarding five or more grains over a nucleus as positive, as has already been extensively described [15,19].

In this study we focused on granulomas with MGC. At least 30 granulomas per lymph node section were screened at random for radio-labelled giant cells. Secondly, to investigate the total number of nuclei present in one single giant cell, serial 5 μm-thick sections from one granuloma, in which one complete MGC could be observed, were used. The total number of nuclei (radio-labelled as well as unlabelled) present in this specific MGC seen in the different sections was counted. For this purpose, three lymph nodes were selected in which the whole bodies of MGC with distinct nuclei were present in the epithelioid cell granulomas.

Table 1a. Quantification of the number of apoptotic bodies per μm^2 granuloma in 17 sarcoidosis lymph nodes.

Lymph node	μm^2 granul.	apopt. bodies	μm^2 observed granul/apopt.b.
24	$63{\cdot}3 \times 10^6$	52	1218×10^3
26	$57{\cdot}1 \times 10^6$	52	1099×10^3
42	$13{\cdot}3 \times 10^6$	15	888×10^3
7	$1{\cdot}7 \times 10^6$	2	871×10^3
32	$14{\cdot}1 \times 10^6$	18	779×10^3
12	$4{\cdot}6 \times 10^6$	6	768×10^3
23	$3{\cdot}6 \times 10^6$	7	518×10^3
3	$4{\cdot}1 \times 10^6$	8	515×10^3
6	$4{\cdot}5 \times 10^6$	9	504×10^3
1	$8{\cdot}1 \times 10^6$	19	427×10^3
19	$7{\cdot}6 \times 10^6$	18	425×10^3
29	$27{\cdot}5 \times 10^6$	106	260×10^3
2	$1{\cdot}7 \times 10^6$	8	218×10^3
10	$6{\cdot}1 \times 10^6$	28	217×10^3
9	$0{\cdot}1 \times 10^6$	1	116×10^3
33	$4{\cdot}9 \times 10^6$	43	114×10^3
16	$1{\cdot}3 \times 10^6$	15	87×10^3

Quantification of apoptosis in 17 sarcoidosis lymph nodes. Quantification of the number of apoptotic bodies per μm^2 granuloma; μm^2 granul, total area of measured granulomatous area; apopt. bodies, number of apoptotic bodies present in the measured granulomatous area; μm^2 observed granul/apop. b., the average μm^2 granuloma area per apoptotic body, sorted on descending range; light-shaded area, lymph nodes in which high numbers of MGC are present.

Morphometry

From our group ($n = 71$) we selected at random lymph node sections from 17 patients. Morphometry was performed using an interactive video overlay-based measuring system (Q-PRODIT, Leica, Cambridge, UK). A 40× plan objective and a 10× ocular were used; the microscopic image was recorded by a charge-coupled device camera and displayed at a final magnification of aproximately 670× on the monitor screen. The border of the investigated lymph node section was traced and the area included was calculated automatically. This was performed on all selected lymph node sections. The percentage of granulomatous area was determined by stereology with a 6-points parallel Weibel grid, using an automatic scanning stage controlled by Q-PRODIT software [25]. Points overlying granuloma, lymphoid tissue or non-granulomatous tissue were counted in 35 randomly selected fields of vision up to a total of 300 points to provide the percentage of granulomatous area. From these data, the total area of the selected granulomas present in one lymph node could be calculated and was expressed in μm^2 (Table 1a: μm^2 granul.).

Quantitation of apoptosis

Part of the 17 lymph node H&E sections described above was selected randomly for assessment of apoptosis. As shown in

Table 1b. Selection of lymph nodes with high numbers of multi-mucleated giant cells (MGC).

Lymph node	μm^2 observed granul/apopt.b.	*n*MGC	tot. surr. area = *n*MGC × 1500 μm^2	*n*MGC + apopt.b.	μm^2 expected granul/apopt.b.
24	1218×10^3	51	76 500	7	$11{\cdot}0 \times 10^3$
42	888×10^3	36	54 000	3	$18{\cdot}0 \times 10^3$
23	518×10^3	16	24 000	1	$24{\cdot}0 \times 10^3$
3	515×10^3	59	88 500	8	$11{\cdot}0 \times 10^3$
19	425×10^3	32	48 000	3	$16{\cdot}0 \times 10^3$
2	218×10^3	17	25 500	3	$8{\cdot}5 \times 10^3$
33	114×10^3	29	43 500	2	$22{\cdot}0 \times 10^3$

Selection of lymph nodes (light-shaded area from Table 1a) with high numbers of MGC. Comparison between the observed density and the expected density of apoptotic bodies per granulomatous area. μm^2 observed granul/apop b., the average granulomatous area per apoptotic body; *n*MGC, total number of MGC (with and without adjacent apoptotic bodies) present in the investigated granulomatous area; tot. surr. area, total granulomatous area: the number of observed MGC, multiplied by their surrounding rim in which an apoptotic body could be present (*n*MGC × 1500 μm^2); *n*MGC + apopt.b, number of MGC with adjacent bodies; μm^2 expected granul/apopt.b., tot. surr.area/(nMGC + apopt.b.).

previous studies [21–23], apoptotic cells can be recognized easily in H&E-stained tissue sections at high magnification. These bodies had to satisfy three of four criteria: (i) fragmentation of nuclear material; (ii) condensation of irregular nuclear material, showing cytoplasmic withdrawal/halo-like effects; (iii) ovoid or spherical-shaped bodies; and (iv) eosinophilia of the cytoplasm. Such bodies were counted in the granulomatous area (see above) at a 500× magnification (40× objective, 12·5× ocular) and expressed per μm^2 granuloma (Table 1a: μm^2 observed granul/apopt. b). From a selection of lymph nodes in which high numbers of MGC were seen, the number of MGC was counted (*n*MGC) and evaluated for adjacent apoptotic bodies (Table 1b: *n*MGC + apopt.b.). Adjacent apoptotic bodies were defined as 'within a rim of 10 μm width surrounding the MGC' (Fig. 1). The average area of a randomly sectioned MGC, as determined by morphometry, covers about 1300 μm^2, so the area of the surrounding rim of this MGC covers about 1500 μm^2. Next, the total area of the rims around all MGC was calculated by multiplying the number of MGC found in the evaluated granulomatous area by 1500 μm^2 (Table 1b: tot. surr. area = *n*MGC × 1500 μm^2). This calculated area was divided by the number of apoptotic bodies adjacent to the MGC (μm^2 expected granul/apopt.b.).

Immunohistochemistry

Fresh operation specimens stored in liquid nitrogen or partly fixed in neutral 4% buffered formaldehyde and embedded in paraffin were used. From these paraffin-embedded tissue blocks, 4 μm sections were stained for immunohistochemistry. Fas, Fas-ligand (Fas-L) and tumour necrosis factor (TNF) were assessed on frozen sections, as described previously [26]. Sections were mounted on poly-L-lysine-coated slides and fixed in acetone. The immunohistochemical procedures (streptavidin–biotin–peroxidase technique) were similar for paraffin and frozen sections, except for peroxidase blocking and antigen retrieval. Briefly, after dewaxing, the endogenous peroxidase activity of the paraffin sections was blocked by incubation for 30 min in 0·3% (vol/vol) hydrogen peroxide in methanol. The slides were heated at 100°C in a 0·01 M citrate buffer (pH 6·0) for 15 min for antigen retrieval. Subsequently, the slides were preincubated

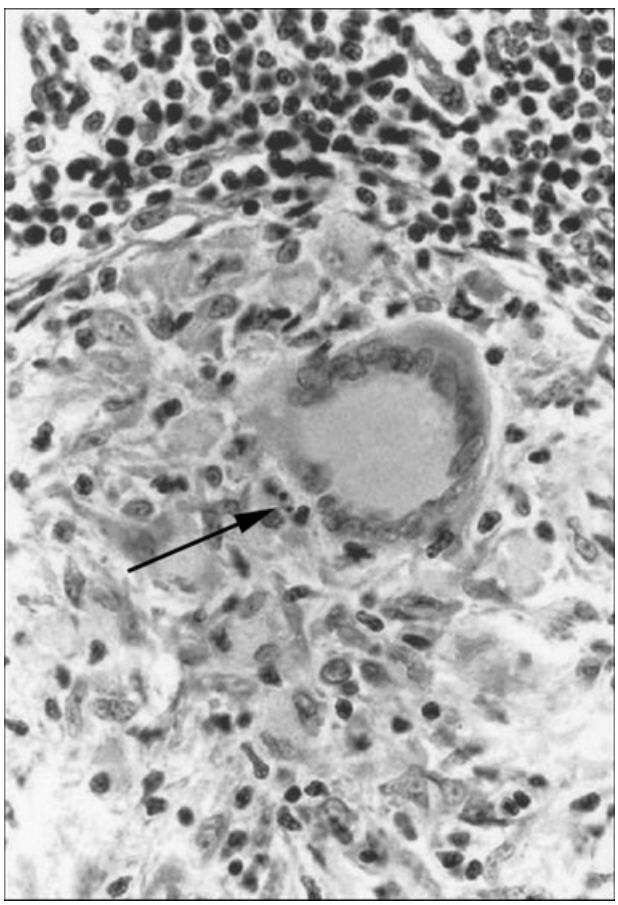

Fig. 1. Granuloma in which an apoptotic body (↖) is seen in the vicinity of a Langhans type giant cell (haematoxylin and eosin staining, ×400).

in normal rabbit serum (1:50; Dako, Glostrup, Denmark) for the mouse monoclonal antibodies and with normal swine serum (1:10 Dako) for the rabbit polyclonal antibodies for 10 min. Thereafter the slides were incubated for 1 h at room temperature with mouse monoclonal antibodies against TNF (1:800; Searle Laboratories, Chicago, IL, USA), Fas-6 (1:2000; gift from Dr Van Aarden from Sanquin, Amsterdam), Fas-L (1:300; Becton Dickinson/Pharmingen/Transduction Laboratory, San Diego, CA, USA), GrB7 (1:500 [27]), GrB11 (1:40), CD44 (1:100, clone U36; Path Vu Med. Centrum, Amsterdam, the Netherlands), perforin (1:100, δG9; Pharmingen, San Diego, CA, USA), CCR-5 (1:50, clone 45531; R&D Systems, Minneapolis, MN, USA), a rabbit monoclonal antibody against active caspase-3 (1:1000; C92-605; Pharmingen) and a rabbit polyclonal antibody against the poly-ADP ribose polymerase (PARP) fragment p85 (1:100; Promega, Madison, WI, USA). Thereafter, the slides were incubated with biotinylated rabbit anti-mouse immunoglobulin (Dako) diluted 1:500 for the mouse monoclonal antibodies and with biotinylated swine anti-rabbit immunoglobulin (Dako) diluted 1:300 for the rabbit antibodies for 30 min at room temperature. The slides were incubated subsequently with avidin–biotinyl–peroxidase complex diluted 1:200 for 60 min. 3,3′-Diaminobenzidine-tetrahydrochloride (DAB; Dako) was used as a chromagen. Between steps, the slides were rinsed for 10 min three times in phosphate-buffered saline (PBS). All sections were counterstained lightly with haematoxylin, dehydrated and mounted. The staining results were graded semiquantitatively from no staining of MGC (−) to intensely stained giant cells (++).

To determine whether apoptotic bodies in close contact with MGC are $CD4^+$, $CD8^+$ or $CD68^+$ cells, a double-staining technique was applied. Co-expression of CD4, CD8 or CD68 with active cleaved caspase 3 was performed on three lymph nodes. Briefly, after deparaffination of the slides endogenous peroxidase activity was blocked by incubation with 0·3% hydrogen peroxide in methanol. Antigen retrieval was performed with Tris ethylenediamine tetraacetic acid (pH 9·0) for 10 min at 100°C in a microwave oven. After cooling, the slides were preincubated with normal goat serum (1:50; Dako) for 10 min. Thereafter the slides were incubated overnight at 4–8°C simultaneously with rabbit anti-cleaved caspase 3 (1:250; Cell Signaling Technology, Beverly, MA, USA) and mouse monoclonal antibodies CD4 (1:10, clone 1F6; Monosan, Uden, the Netherlands), CD8 (1:50, clone 8/144; Dako) or CD68 (1:800, clone KP1; Dako). Thereafter the slides were incubated with Power Vision Plus (Immunologics, Duiven, the Netherland) supplemented with biotinylated goat anti-mouse immunoglobulin (1:500; Dako) for 30 min at room temperature. The slides were incubated subsequently with streptavidin–alkaline phosphatase (Roche, Basel Switzerland) diluted 1:100 for 60 min. First, the DAB (Dakocytomation, Glostrup, Denmark) was used for visualization according to the manufacturer's procedure. Thereafter the alkaline phosphatase was visualized by naphthol AS MX and Fast Blue BB for 30–45 min. Between steps, the slides were rinsed for 10 min three times in PBS. All sections were counterstained lightly with haematoxylin, dehydrated and mounted with aquamount (VWR International Ltd, Poole, Dorset, UK).

Data analysis

Statistical analyses (linear regression analysis, signed-rank test) were performed using SPSS software (SPSS, Chicago, IL, USA), regarding *P*-values below 0·05 as significant.

Results

The MGC investigation

Non-caseating epithelioid cell granulomas were found in 71 lymph nodes from 32 female and 39 male sarcoidosis patients, but fibrinoid necrosis or hyalinization was hardly present. In these granulomas a wide variation in numbers of both types of MGC could be seen: eight nodes did not show any MGC at all, in four nodes only a LH-MGC was incidentally seen. The other nodes contained a variable number of both types of giant cells. Small as well as large giant cells could be observed, the latter sometimes with an impressive number of nuclei (>> 100, see below). The numbers of LH-MGC or FB-MGC present in all the measured granulomas in the lymph node section were calculated as a percentage of LH-MGC or FB-MGC and were compared with each other. Regression analysis points to a relationship between LH-MGC and FB-MGC (Fig. 2; $r = 0{\cdot}735$).

The MGC radio-labelling

In sections radio-labelled with [^{3}H]-thymidine, no single-labelled nucleus could be detected in any MGC (Table 2). Radio-labelled macrophages and epithelioid cells were nevertheless seen in the same granulomas (Fig. 3a), underlining that [^{3}H]-thymidine labelling experiments were technically successful. In addition, mitotic figures were seen incidentally in these granulomas, but never in MGC. Secondly, RNA synthesis as measured by means of [^{3}H]-uridine incorporation was clearly present in most of the MGC present in nodes, as mentioned above. A large variation in labelling was observed. Twenty-three MGC showed only + radio-labelled nuclei, but 26 of the MGC (33%) showed labelled as well as unlabelled nuclei (±) in the same giant cell (Table 2 and Fig. 3b). The remaining 29 giant cells showed no labelling (−) at all.

Serial sections were studied from three of these nodes (58, 60 and 66), allowing evaluation of the whole body of LH-MGC or FB-MGC. In this manner, the exact number of [^{3}H]-uridine-labelled nuclei could be enumerated among the total number of nuclei within one specific MGC. Lymph node 58, in which MGC (LH6) with 104 (40 unlabelled– and 64 [^{3}H]-uridine+ labelled nuclei) and lymph node 66, in

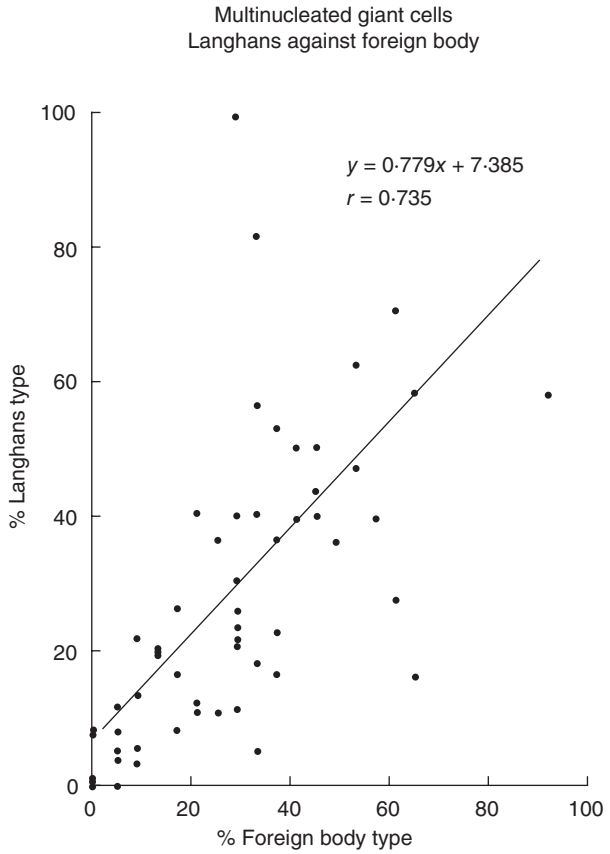

Fig. 2. Regression analysis of Langans type (LH)- against foreign body type (FB)-multi-nucleated giant cells (MGC). % Langhans type = [the number of LH-MGC/total number of multinucleated giant cells (MGC)] × 100; % foreign body type = (the number of FB-MGC/total number of MGC) × 100.

which MGC (FB1) with 239 nuclei (with 48 unlabelled– and 191+ labelled nuclei) were seen. Within a lymph node, a wide variation existed between the rates of labelled nuclei from both types of giant cells (from 15% to 96%), as seen in the evaluated granulomas in lymph node 60.

Apoptosis

Apoptotic bodies could be seen clearly in epithelioid cell granulomas in H&E-stained sections (Fig. 1). The frequency of these bodies in lymph nodes varied widely. Some nodes incidentally displayed an apoptotic body, while in other nodes relatively high numbers of bodies were seen (Table 1a: lymph nodes 24, 26 and 29). To compare these data, the number of these bodies as observed in one lymph node section was recalculated in relation to the average granuloma area (Table 1a, last column). These values (μm^2 observed granul/apopt.b.) ranged from 1218 to 87×10^3.

These bodies were present remarkably often directly adjacent to MGC (Fig. 1). Therefore, we selected seven lymph nodes from this group in which many MGC were present (Table 1b) to number the apoptotic bodies around the MGC. The observed frequencies of these bodies (second column) were significantly higher than expected on the average number of apoptotic bodies in the granulomatous area (sixth column; signed-rank test, $P = 0{\cdot}005$). In addition, no apoptotic bodies were seen lying within a MGC.

Immunohistochemistry of apoptosis

Mononuclear histiocytes within the granulomas showed variable staining, from negative to moderately positive, for Fas-L, caspase-3, p85, perforin, GrB7 and GrB-11, while TNF and Fas displayed more staining. MGC staining for TNF and Fas-L varied widely (sometimes within a single lymph node) from negative to strongly positive. More giant cells were stained for caspase-3, TNF and GrB11 and displayed the same spectrum mentioned above. Granzyme B-positive MGC were seen, showing a finely granular pattern. MGC displayed more TNF activity compared with the overall granuloma staining (Table 3a). A high number of giant cells (66%) with caspase-3 activity were noted, while fewer $p85^+$ cells were seen. However co-expression of caspase-3 and p85 could be demonstrated in individual MGC by serially sectioned granulomas. About 60% of the MGC were positive for TNF and Fas-L, while strong expression was sometimes noted. Fas-L was expressed more on MGC membranes (Fig. 4a), compared with the lower expression seen in granulomas ($P = 0{\cdot}0001$). On the other hand, Fas staining showed the reverse pattern ($P = 0{\cdot}0166$). In addition, in the neighbourhood of these giant cells Fas^+ lymphocytes were observed only incidentally. CCR-5^+ was expressed over all the granulomas, but MGC showed hardly any positivity for this receptor (Fig. 4b). It was striking that in a number of MGC, CD44 expression was confined only to the outer cytoplasmic rim (Fig. 4c). Apoptotic bodies in contact with these MGC were always negative for CD44.

In double staining, co-expression of caspase-3^+/$CD4^+$ (Fig. 4d) and caspase-3^+/$CD68^+$ bodies in close contact with MGC were numbered, but no caspase-3^+/$CD8^+$ cells were found (Table 3b).

Discussion

In inflammatory diseases organized epithelioid cell granulomas often contain MGC, and they may be involved actively in destruction [10]. Some controversy exists with regard to the differentiation of FB and LH types of giant cells as to whether they derive by fusion or proliferation and non-disjunction. Van Furth [1] proposed that such MGC in granulomas are formed by fusion of macrophages rather than by division and non-disjunction of cells. However, DNA synthesis with nuclear division in giant cells has also been described [4–8]. Fusion of macrophages resulting in unordered FB-MGC or ordered LH-MGC has also been reported [1,2,5,28–30]. FB-MGC and LH-MGC do not

Table 2. Radionucleotide incorporation in sarcoidosis lymph nodes.

		[^{3}H]-labelled multi-nucleated giant cells													
		[^{3}H]-thymidine				[^{3}H]-uridine					[^{3}H]-uridine				
Lymph node	d MGC	*n*	–	±	+	*n*	–	±	(%)	+	MGC	Sections	–	+	(per)
58	0·45	7	7	0	0	12	6	5	(42)	1	LH6	6	40	64	61
											LH7	7	64	26	24
60	0·37	12	12	0	0	11	7	3	(27)	1	LH1	6	3	75	96
											LH2	7	17	43	72
											LH6	7	17	35	65
											FB4	4	25	18	42
											FB5	5	58	10	15
56	0·35	17	17	0	0	26	7	8	(31)	11	nt	–	–	–	–
57	0·31	nt				10	4	4	(40)	2	nt	–	–	–	–
66	0·23	25	25	0	0	14	3	4	(29)	7	FB1	9	48	191	80
											LH1	5	81	31	28
53	0·11	7	7	0	0	3	1	1	–	1	nt	–	–	–	–
59	0·07	$\underline{3}_+$	$\underline{3}_+$	$\underline{0}_+$	$\underline{0}_+$	$\underline{2}_+$	$\underline{1}_+$	$\underline{1}_+$	–	$\underline{0}_+$	nt	–	–	–	–
Number of MGC		71	71	0	0	78	29	26	(33)	23	nt	–	–	–	–

Radio nucleotide incorporation in sarcoidosis lymph nodes. Lymph node, sarcoidosis lymph node obtained from patient no. X; d MGC, density of giant cells per granulomas: (number of LH-MGC as well as FB-MGC)/30 granulomas; *n*, total number of observed multi-mucleated giant cells (MGC) per lymph node; –, number of MGC without any RNA or DNA synthesizing nuclei; ±, number of MGC with radio-labelled as well as unlabelled nuclei in the same giant cell; +, number of MGC in which all nuclei are labelled; (%), percentage of MGC which contains [^{3}H]-uridine-labelled as well as unlabelled nuclei; nt, not tested; LH7, seventh evaluated Langhans MGC as observed in seven successive sections from lymph node 58; FB4, fourth foreign body MGC as observed in four successive sections from node 60; sections, number of serial sections of the same MGC; (per), percentage of radiolabelled nuclei in one MGC.

represent distinct cell types, but rather different degrees of nuclear and cytoplasmic organization [11]. LH-MGC is often seen in sarcoidosis or tuberculosis, while FB-MGC are found mainly in infectious or foreign body granulomas, but these types of MGC are by no means specific for a certain type of disease [18,31]. In contrast with sarcoidosis other MGC-related diseases do not, as a rule, lead to mediastinal lymph node sampling. Therefore, we focused on human sarcoid MGC because little is known about their formation and behaviour *in vivo*. Quantitation of LH-MGC and FB-MGC was performed retrospectively in granulomas from a large number of subclavicular and mediastinal lymph nodes of established sarcoidosis patients. In the present study regression analysis showed a relationship between the number of LH-MGC and FB-MGC, so an increase of LH-MGC in the granulomatous lymph node is accompanied generally by an increase of FB-MGC.

Proliferation of giant cells in animals has also been described in the literature. Prieditis and Adamson injected [^{3}H]-thymidine in mice with induced pulmonary asbestosis, fibrosis or silicosis [8]. In their bronchial lavages, radio-labelled macrophages were recovered but no radio-labelled MGC were seen, so macrophage proliferation preceded MGC formation, which takes place by means of fusion. However, intravenous injection of [^{3}H]-thymidine in rats showed a majority of LH-MGC in which all nuclei were labelled. Labelled as well as unlabelled nuclei were found in other giant cells, suggesting a fusion process [3]. In sarcoidosis, the human granulomatous disorder, this process still

Table 3a. Distribution of apoptosis-related cytokines/enzymes/ligands between granulomas and multi-mucleated giant cells (MGC).

	Granuloma			MGC		
	% –	% +	% ++	% –	% +	% ++
TNF-α	52	46	1·6	37	59	4·3
Fas	37	62	0·9	87	13	0·0
Fas-L	68	32	0·0	36	53	10·0
Casp-3	70	30	0·0	34	66	0·0
P85	56	44	0·0	55	45	0·0
Perforin	81	19	0·0	55	45	0·0
GrB7	56	44	0·0	57	43	0·0
GrB11	65	35	0·0	26	74	0·0

Distribution of apoptosis-related cytokines/enzymes/ligands between granulomas and MGC. TNF, tumour necrosis factor; casp-3, caspase-3; Fas-L, Fas ligand.

Table 3b. Double staining of multi-mucleated giant cells (MGC) adhering apoptotic bodies in three lymph nodes.

Lymph node	*n*MGC	Casp-3$^+$/CD4$^+$	Casp-3$^+$/CD8$^+$	Casp-3$^+$/CD68$^+$
34	65	1	0	1
42	77	2	0	3
68	245	5	0	2

Double-stained apoptotic bodies in three lymph nodes. Numbers of MGC with adjacent double-stained apoptotic bodies; *n*MGC, total number of observed MGC; casp-3$^+$/CD4$^+$, number of (double-stained) caspase-3$^+$ and CD4$^+$ apoptotic bodies.

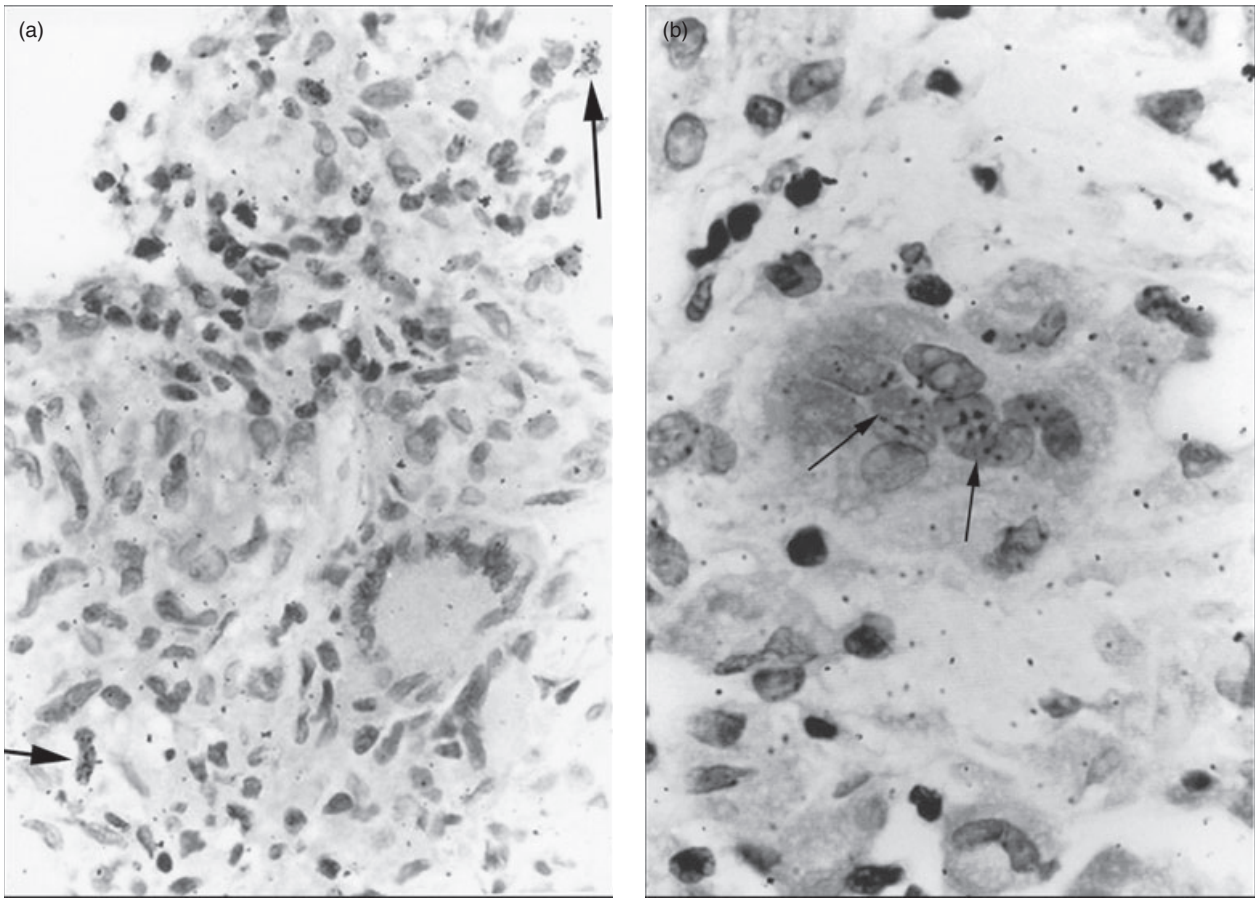

Fig. 3. (a) Light microscopic appearance of a sarcoidosis lymph node section labelled with [^{3}H]-thymidine. In the epithelioid cell granuloma two radio-labelled mononuclear cells (↖) are seen, while a Langhans giant cell showed no radio-labelling [haematoxylin and eosin staining (H&E), ×400]. (b) In a granuloma section labelled with [^{3}H]-uridine, a foreign body type giant cell is clearly visible in which some nuclei are radio-labelled (↖) (H&E staining, ×1000).

remained questionable, although a mitotic figure could be found incidentally in a giant cell in human granulomatous tissue [31].

To resolve this controversy, we reassessed [^{3}H]-radio-labelled sections from earlier studies [19,20]. Although immunostaining for proliferating related antigens such as Ki-67 labelling is now often used to assess proliferation, [^{3}H]-radio labelling remains the gold standard in cell biology [32,33]. No nuclei in MGC were labelled during 3 h incubation with [^{3}H]-thymidine, indicating a lack of DNA synthesizing properties for such MGC. In addition, we have already reported [^{3}H]-thymidine-labelled alveolar macrophages (2–19%) from sarcoidosis patients [34], but no [^{3}H]-thymidine-labelled MGC were found in evaluating the same lavages.

From our serial lymph node sections incubated with [^{3}H]-thymidine, in which whole MGC could be enumerated, no single nucleus could be found labelled with [^{3}H]-thymidine. The absence of labelled MGC was not an artefact caused by the described incubation technique, but a real phenomenon. This could be demonstrated clearly in control experiments with [^{3}H]-uridine labelling [19]. The nuclei of granulomatous MGC demonstrated variable degrees of labelling. This can lead only to the conclusion that, in human sarcoidosis disorder, MGC derive by cell fusion and not by division/non-disjunction. Furthermore, such MGCs as observed in these nodes are probably in variable phases of life; therefore, we believe that our data confirm the proposed sequence from macrophage via epithelioid cell formation leading to LH-MGC and FB-MGC and a process of decay.

In response to foreign bodies by means of receptors (such as DC-Stamp, CD44, CCR-5, etc.), fusion which leads up to MGC [2,3,5,8,35] is often induced. However, in sarcoidosis there are only reports about CD44. Interestingly, CD44 and its putative cell surface ligand, described in the process of fusion and differentiation of rat macrophages towards MGC [36], was also present on the surface of our sarcoid MGC. The inflammation-specific homing receptor CCR-5, involved in the traffic of T cells to the inflammatory area, was expressed clearly in granulomas in the present study, but not in MGC. Therefore, persistence of the granulomatous inflammation because of increased CCR-5 in these

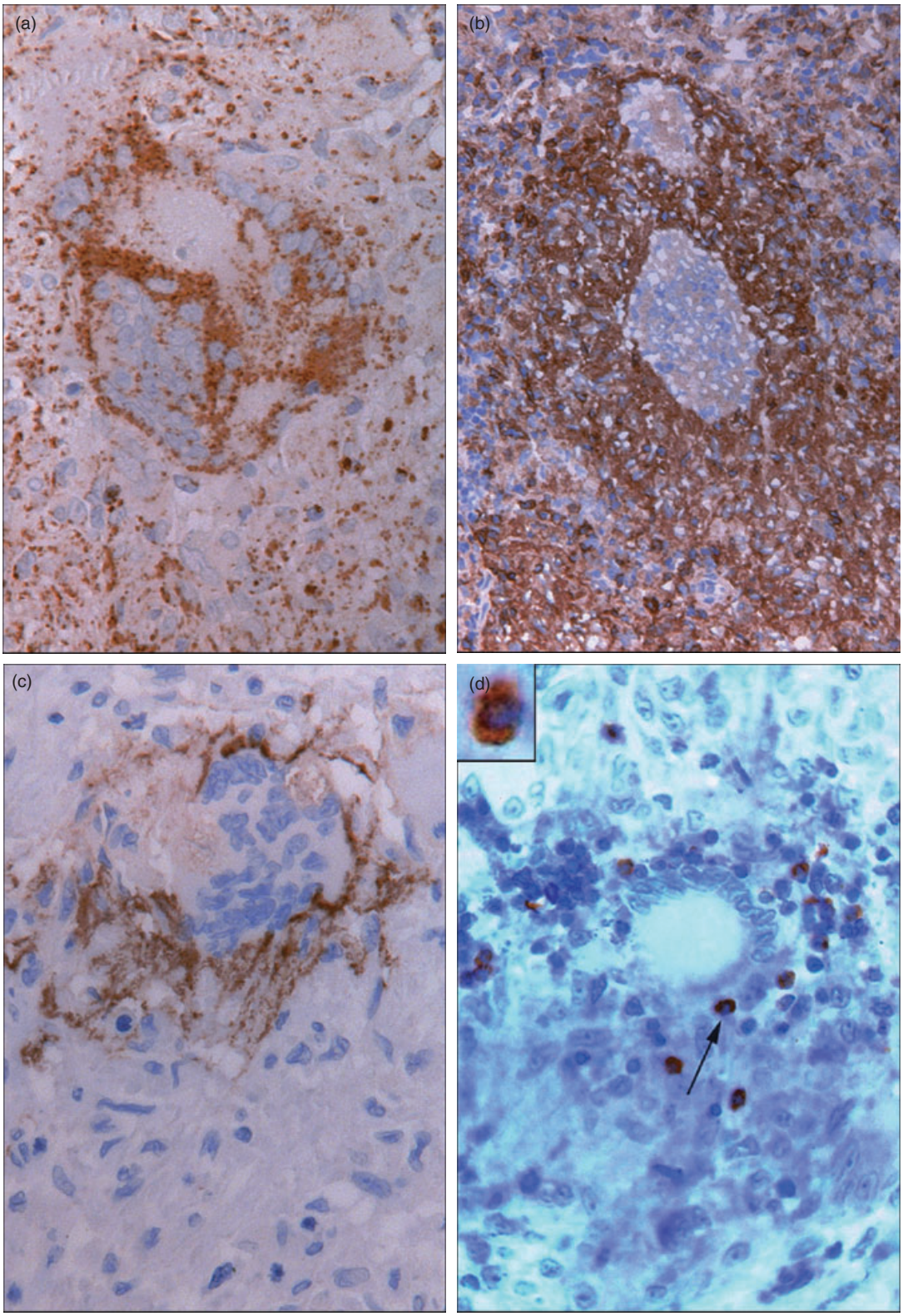

Fig. 4. (a) Giant cell stained for Fas-ligand (Fas-L). Centre of the cell with no staining while the rim of the cell is Fas-L positive. Around the multi-nucleated giant cells (MGC) some Fas-L$^+$ staining is also visible (Fas-L immunostaining, ×630). (b) CCR-5$^+$ sarcoid granulomas within two CCR-5-negative FB-MGC (CCR-5 immunostaining, ×200). (c) Cell membrane of MGC stained positively for CD44. A CD44-negative apoptotic body is also visible (CD44 immunostaining, ×220). (d) LH-MGC in close contact with an apoptotic body (↖). Inset (2·4×): Co-expression of caspase-3 (brown) and CD4 (blue) of this body is clearly visible (caspase-3/CD4 immuno-double-staining, ×400).

granulomas [37] may result in an unsettled Fas/Fas-L system [38,39] in combination with the low number of apoptotic cells as are present in such sarcoid inflammatory reactions [21]. In addition, Toll-like receptors (TLR) recognizing microbiological products [40] involved in the immune response may be of importance in sarcoidosis. Veltkamp *et al.* [41,42] studied such receptors in peripheral blood of sarcoidosis patients. However, the reported results are conflicting, which makes it unlikely that TLR play a major role in sarcoidosis. We have therefore not performed TLR immunohistochemistry in the present study.

With regard to the MGC turnover, apoptosis [43,44], which becomes morphologically visible in a more advanced phase, was studied [22]. H&E staining was used to identify apoptotic bodies, as this correlates with DNA methods [45] and is reproducible [23]. Apoptosis was seen rarely in the granulomas of our sarcoidosis patients, also reported by Petzmannn [46]. Our measurement of the density of these bodies (Table 1a) confirms the observation of Cree [21], who calculated 0–9 apoptotic cells/mm^2 granulomatous tissue. Screening our H&E sections showed that a number of MGC had adjacent apoptotic bodies relatively often. Using morphometry we demonstrated that close to MGC significantly more of these bodies were seen, compared with the frequency seen over the whole granulomatous area. This led us to the hypothesis that MGC may induce apoptosis, or are at least involved in this process. Although negative staining for caspase-3 in lung biopsies was reported [47], some staining for caspase-3 as well as p85 was noted on our lymphoid granulomas, and confirmed clearly our H&E findings that apoptosis is seen remarkably often around MGC. Serial slides stained with caspase-3 and p85 [47] showed individual MGC positive for both proteins. To differentiate the apoptotic cells further, we performed double staining with CD4/caspase-3, CD8/caspase-3 and CD68/caspase-3. This clarified that the caspase-3$^+$ apoptotic bodies around the MGC were CD4$^+$ lymphocytes or CD68$^+$ macrophages. No caspase-3/CD8-positive apoptotic cells were found close to MGC, which is in line with the finding that CD8$^+$ lymphocytes are found only in the periphery of granulomas [48].

Apoptosis can be mediated by cell surface receptor/ligand interaction or by soluble factors. A preliminary investigation was perfromed by screening for expression of TNF, Fas and Fas-L. Cell surface receptor-ligands such as Fas and TNF belong to the tumour necrosis family [38]. Cytotoxic T lymphocytes (CTL) can induce an apoptotic signal by means of Fas or by exocytosis of GrB and perforin [49]. Granzyme B, produced by CTL, enters the target cell through perforin-derived channels and activates caspase-3, which cleaves the PARP into a p85 protein fragment [50] and leads to apoptosis. Soluble factors involved in the granzyme-, perforin- or CD95- pathway (such as Fas, Fas-L and TNF), which mediate apoptosis, down-regulate T cell activation in the early phases of apoptosis. The Fas/FasL balance [38,51,52] observed in our granulomas was quite different compared with this balance as seen on our MGC (Table 3a). A number of MGC expressed Fas-L, just as reported in MGC from tuberculoid granulomas [53], while expression of Fas$^+$ on CD4$^+$ lymphocytes was seen around these MGC. MGC showed a remarkable Fas-L and GrB7 staining of only the outer cytoplasmic rim, also demonstrated previously by Fayyazi *et al.* [54]. This staining pattern was consistent, as seen in serial sections of the same MGC. We believe that this is not an artefact but a genuine phenomenon, related possibly to secretion of the above proteins. We studied previously [48] the regulatory role of T cells in this process, finding that the CD4/CD8 ratio within the central and peripheral areas of granulomas differed, which suggests an immunological dynamic process, and the abundance of CD4$^+$ cells within granulomas points to a dominant role of these T cells in sarcoidosis granulomas.

In conclusion, we show that giant cells in sarcoidosis arise by means of fusion of epithelioid cells and not by division/non-disjunction. Further, we find indications that giant cells in sarcoidosis may induce apoptosis of the nearby CD4$^+$ lymphocytes and macrophages.

Acknowledgements

We thank Professor Dr J. Stam for access to the lymph nodes and to their records. We are very grateful to Dr D. Dukers for his advice, Dr A. Kummer for his critical comments on the manuscript and are indebted to Dr van Vliet for a generous supply of monoclonal anti-human perforin and the excellent technical help of Mrs T. H. Tadema.

References

1 van Furth R, Cohn ZA, Hirsch JG, Humphry JH, Spector WG, Langevoort HL. The mononuclear phagocyte system. A new classification of macrophages, monocytes and their precursor cells. Bull WHO 1972; **46**:845–52.
2 Chambers TJ. Multinucleate giant cells. J Pathol 1978; **126**:125–48.
3 Thoenes W, Sonntag W, Heine WD, Langer KH. Cell fusion as a mechanism for the formation of giant cells (Langhans' type). Autoradiographic findings in autoimmune tubulo-interstitial nephritis of the rat. Virchows Arch B 1982; **41**:45–50.
4 Ryan GB, Spector WG. Macrophage turnover in inflamed connective tissue. Proc R Soc Lond B Biol Sci 1970; **175**:269–92.
5 Mariano M, Spector WG. The formation and properties of macrophage polykaryons (inflammatory giant cells). J Pathol 1974; **113**:1–19.
6 Dreher R, Keller HU, Hess MW, Roos B, Cottier H. Early appearance and mitotic activity of multinucleated giant cells in mice after combined injection of talc and prednisolone acetate. Lab Invest 1978; **38**:149–56.
7 Drexler HG, Gignac SM, Hoffbrand AV, Minowada J. Formation of multinucleated cells in a Hodgkin's disease derived cell line. Int J Cancer 1989; **43**:1083–90.
8 Prieditis H, Adamson IY. Alveolar macrophage kinetics and multinucleated giant cell formation after lung injury. J Leukoc Biol 1996; **59**:534–38.

9 Williams GT, Jones Williams W. Granulomatous inflammation – a review. J Clin Pathol 1983; **36**:723–33.
10 Cain J, Kraus B. Significance and function of multinucleate giant cells in De Quervain's thyroiditis. Diagn Histopathol 1983; **6**:181–93.
11 Rigby PJ, Papadimitriou JM. Cytoskeletal control of nuclear arrangement in Langhans multinucleate giant cells. Pathol 1984; **143**:17–29.
12 van der Rhee HJ, Hillebrands W, Daems WTh. Are Langhans giant cells precursors of foreign-body giant cells? Arch Derm Res 1978; **263**:13–21.
13 Smetena K. Multinucleate foreign-body giant cell formation. Exp Mol Pathol 1987; **4**:258–65.
14 McNally AK, Anderson JM. Interleukin-4 induces foreign body giant cells from human monocytes/macrophages. Am J Pathol 1995; **147**:1487–99.
15 Gerberding K, Yoder MC. *In vitro* comparison of multinucleated giant cell formation from human umbilical cord and adult peripheral blood mononuclear phagocytes. Pediatr Res 1993; **33**:19–26.
16 Liu ZX, Noguchi M, Hiwatashi N, Toyota T. Monocyte aggregation and multinucleated giant-cell formation *in vitro* in Crohn's disease. The effect of cell adhesion molecules. Scand J Gastroenterol 1996; **31**:706–10.
17 Okamoto H, Mizuno K, Horio T. Langhans-type and foreign-body-type multinucleated giant cells in cutaneous lesions of sarcoidosis. Acta Derm Venereol 2003; **83**:171–74.
18 van Maarssveen ACMTh, Veldhuizen RW, Stam J, Alons CL, Mullink H. A quantitative histomorphologic analysis of lymph node granulomas in sarcoidosis in relation to radiological stage I and II. J Pathol 1983; **139**:441–53.
19 van Maarsseveen ACMTh, van der Gaag RD, Stam J. Measurements of RNA-synthesis in granulomas, localized in lymph nodes of sarcoidosis patients. Virchows Arch 1982; **40**:273–77.
20 van der Gaag RD, van Maarsseveen ACMTh, Broekhuizen-Davies JM, Stam J. Application of *in vitro* techniques to determine proliferation in human sarcoid lymph nodes. J Pathol 1983; **139**:239–45.
21 Cree IA, Nurbhai S, Milne G, Beck JS. Cell death in granulomata: the role of apoptosis. J Clin Pathol 1987; **40**:1314–19.
22 Kerr JFR, Gobé GC, Winterford CM, Harmon BV. Anatomical methods in cell death. In: Schwartz LM, Osborne BA, eds. Methods Cell Biol. New York: Academic Press, 1995; 46:1–27.
23 van de Schepop HA, de Jong JS, van Diest PJ, Baak JP. Counting of apoptotic cells: a methodological study in invasive breast cancer. J Clin Pathol Mol Pathol 1996; **49**:M 214–17.
24 Honma T, Hamasaki T. Ultrastructure of multinucleated giant cell apoptosis in foreign-body granuloma. Virchows Arch 1996; **428**:165–76.
25 van Hensbergen Y, Luykx-de Bakker SA, Heideman DAM, Meijer GA, Pinedo HM, van Diest PJ. Rapid stereology based quantitative immunohistochemistry of dendritic cells in lymph nodes: a methodological study. Anal Cell Pathol 2001; **22**:143–49.
26 de Jong JS, van Diest PJ, van der Valk P, Baak JP. Expression of growth factors, their receptors and growth inhibiting factors in invasive breast cancer II. Correlations with proliferation and apoptosis. J Pathol 1998; **184**:53–7.
27 Kummer JA, Kamp AM, van Katwijk M *et al.* Production and characterization of monoclonal antibodies raised against recombinant human granzymes A and B showing cross reactions with the natural proteins. J Immunol Methods 1993; **63**:77–83.
28 Murch AR, Grounds MD, Marchall CA, Papadimitriou JM. Direct evidence that inflammatory multinucleate giant cells form by fusion. J Pathol 1982; **137**:177–80.
29 Lan HY, Nikolic-Paterson DJ, Mu W, Atkins RC. Local macrophage proliferation in multinucleated giant cell and granuloma formation in experimental Goodpasture's syndrome. Am J Pathol 1995; **147**:1214–20.
30 Unanue ER. Cooperation between mononuclear phagocytes and lymphocytes in immunity. N Engl J Med 1980; **303**:1153–56.
31 Cain H, Kraus B. Multinucleated giant cells in Granulomas. Virchows Arch 1980; **385**:309–33.
32 Oesterle EC, Cunningham DE, Westrum LE, Rubel EW. Ultrastructural analysis of [3H]thymidine-labeled cells in the rat utricular macula. J Comp Neurol 2003; **463**:177–95.
33 Kamel OW, Franklin WA, Ringers JC, Meyer JS. Thymidine labeling index and Ki-67 growth fraction in lesions of the breast. Am J Pathol 1989; **134**:107–13.
34 van Maarsseveen T, Eckert H, de Groot J *et al.* Proliferative capacity of mononuclear cells in the human lung. J Immunol Methods 1991; **143**:95–102.
35 Yagi M, Miyamoto T, Sawatani Y *et al.* DC-STAMP is essential for cell–cell fusion in osteoclasts and foreign body giant cells. J Exp Med 2005; **202**:345–51.
36 Cui W, Ke JZ, Zhang Q, Ke HZ, Chalouni C, Vignery A. The intracellular domain of CD44 promotes the fusion of macrophages. Blood 2006; **107**:796–805.
37 Capelli A, DI Stefano A, Lusuardi M, Gnemmi I, Donner CF. Increased macrophage inflammatory protein-1α and macrophage inflammatory protein-1β levels in bronchoalveolar favage fluid of patients affected by different stages of pulmonary sarcoidosis. Am J Respir Crit Care Med 2002; **165**:236–41.
38 Nagata S, Goldstein P. The Fas death factor. Science 1995; **267**:1449–56.
39 Spagnolo P, Renzoni EA, Wells AU *et al.* C-C chemokine receptor 5 gene variants in relation to lung disease in sarcoidosis. Am J Respir Crit Care Med 2005; **172**:721–8.
40 Atkinson TJ. Toll-like receptors, transduction-effector pathways, and disease diversity: evidence of an immunobiological paradigm explaining all human illness? Int Rev Immunol 2008; **27**:255–81.
41 Veltkamp M, Grutters JC, van Moorsel CH, Ruven HJ, van den Bosch JM. Toll-like receptor (TLR) polymorphism Asp299Gly is not associated with disease course in Dutch sarcoidosis patients. Clin Exp Immunol 2006; **145**:215–8.
42 Veltkamp M, Wijnen PA, van Moorsel CH *et al.* Linkage between Toll-like receptor (TLR)-2 promotor and intron polymorphism: functional effects and relevance to sarcoidosis. Clin Exp Immunol 2007; **149**:453–62.
43 Schmied M, Breitschopf H, Gold R *et al.* Apoptosis of T lymphocytes in experimental autoimmune encephalomyelitis. Evidence for programmed cell death as a mechanism to control inflammation in the brain. Am J Pathol 1993; **143**:446–52.
44 Berke G The CTL's kiss of death. Cell 1995; **81**:9–12.
45 Hawkins NJ, Lees J, Ward RL. Detection of apoptosis in colorectal carcinoma by light microscopy and *in situ* end labelling. Anal Quant Cytol Histol 1997; **19**:227–32.
46 Petzmann S, Maercker C, Markert E *et al.* Enhanced proliferation and decreased apoptosis in lung lavage cells of sarcoidosis patients. Sarcoidosis Vasc Diffuse Lung Dis 2006; **23**:190–200.
47 Alam A, Cohen LY, Aouad S, Sekaly RP. Early activation of caspases during T lymphocyte stimulation results in selective substrate cleavage in non apoptotic cells. J Exp Med 1999; **190**:1879–90.

48 van Maarsseveen ACMTh, Mullink H, Alons C, Stam J. The distribution of T lymphocyte sub-sets in different portions of sarcoid granulomas: immunohistologic analysis with monoclonal antibodies. Hum Pathol 1986; **17**:493–500.
49 Barry M, Heibein JA, Pinkoski MJ *et al.* Granzyme B short-circuits the need for caspase 8 activity during granule-mediated cytotoxic T-lymphocyte killing by directly cleaving. Bid Mol Cell Biol 2000; **20**:3781–94.
50 Casiola-Rosen L, Nicholson DW, Chong T *et al.* Apopain/CPP32 cleaves proteins that are essential for cellular repair: a fundamental principle of apoptotic death. J Exp Med 1996; **183**:1957–64.
51 Kunitake R, Kuwano K, Miyazaki H, Hagimoto N, Nomoto Y, Hara N. Apoptosis in the course of granulomatous inflammation in pulmonary sarcoidosis. Eur Respir J 1999; **13**:1329–37.
52 Shikuwa C, Kadota J, Mukae H *et al.* High concentrations of soluble Fas ligand in bronchoalveolar lavage fluid of patients with pulmonary sarcoidosis. Respir 2002; **69**:242–6.
53 Mustafa T, Bjune TG, Jonsson R, Pando RH, Nilsen R. Increased expression of fas ligand in human tuberculosis and leprosy lesions: a potential novel mechanism of immune evasion in mycobacterial infection. Scand J Immunol 2001; **54**:630–9.
54 Fayyazi A, Eichmeier B, Soruri A *et al.* Apoptosis of macrophages and T cells in tuberculosis associated caseous necrosis. J Pathol 2000; **191**:417–25.